

Effect of Heat Treatment on the Microstructure and Hardness of 17Cr-0.17N-0.43C-1.7 Mo Martensitic Stainless Steel

S. Chenna Krishna, Narendra Kumar Gangwar, Abhay K. Jha, Bhanu Pant, and Koshy M. George

(Submitted May 29, 2014; in revised form November 30, 2014; published online February 18, 2015)

The microstructure and hardness of a nitrogen-containing martensitic stainless steel were investigated as a function of heat treatment using optical microscopy, electron microscopy, amount of retained austenite, and hardness measurement. The steel was subjected to three heat treatments: hardening, cryo treatment, and tempering. The hardness of the steel in different heat-treated conditions ranged within 446–620 HV. The constituents of microstructure in hardened condition were lath martensite, retained austenite, $M_{23}C_6$, M_7C_3 , MC carbides, and M(C,N) carbonitrides. Upon tempering at 500 °C, two new phases have precipitated: fine spherical Mo_2C carbides and needle-shaped Cr_2N particles.

Keywords carbides, hardness, heat treatment, martensitic stainless steel

melting by injecting nitrogen gas, powder metallurgy etc. (Ref 8, 9). With this background, a nitrogen-containing MSS was designed, melted, and processed. The aim of the present study is to establish relationship between microstructure and hardness of the steel after different heat treatments.

1. Introduction

High-carbon martensitic stainless steels (MSSs) find applications in the aerospace industry as bearings because of high hardness and good corrosion resistance (Ref 1). Stainless steels based on Fe-Cr-C-Mo system are widely used for such application for following reasons: (i) Carbon imparts solid solution strengthening and dispersion strengthening by formation of carbides; (ii) 12% Cr makes steel stainless by forming a thin, coherent film of chromium oxide on the surface and (iii) Mo improves the pitting corrosion resistance of the steel (Ref 2). Currently, AISI 440C (Fe-17%Cr-1%C-1.2%Mo) steel is being used as cryogenic bearings because of inherent high hardness coupled with enhanced wear and corrosion resistance (Ref 3, 4). Nevertheless, the presence of high carbon leads to formation of large eutectic carbides ($M_{23}C_6$ and M_7C_3) which are detrimental to the fatigue life of the bearings (Ref 5).

Efforts have gone into the design of new grades of stainless steel with refined carbides and retaining the corrosion resistance to improve fatigue life. The outcome of the research is series of steels like Cronidur 30, Pyrowear 675, CSS-42L, XD15NW, 13Cr-SS (Ref 6, 7). All the listed steels have hardness in the range of 54–60 HRC at room temperature in hardened and tempered condition. However, steels with nitrogen showed microstructure with finer carbides aiding to better fatigue life (Ref 7). Even though it is advantageous to have nitrogen, it is rather difficult to add nitrogen in MSS due to its low solubility (Ref 8). Several special techniques were used for producing nitrogen MSS like pressure electro slag melting, induction

2. Experimental Procedure

A 15 kg melt of the steel was taken by vacuum induction melting under positive pressure of nitrogen as the nitrogen content aimed is higher than 0.1 wt.%. High carbon ferrochrome and high nitrogen ferrochrome were used as a source of nitrogen and carbon, respectively. The remaining elements were added as pure metals. The melting was done in a magnesia crucible and poured into a mild steel mold. The chemical composition of the steel was Fe-17Cr-0.17 N-0.43C-1.7Mo-0.12Nb-0.20 V (wt.%). The cast ingot was homogenized at 1080 °C for 8 h followed by air cooling. This ingot was subsequently hot worked (forging and rolling) in the temperature range (1080–950 °C) to produce a plate of 6 mm thickness. Samples cut from plate were subjected to hardening, cryo treatment, and tempering. Hardening was performed in the temperature range of 950–1100 °C for 0.5 h and air cooled. Cryo treatment was performed using a cryo chamber at –80 °C for holding time of 2 h and warmed in the same chamber to reach ambient temperature. This was followed by tempering at four temperatures for 2 h viz., 180, 250, 500, and 525 °C. The hardness of the heat-treated samples was measured using a universal hardness tester with a test load and dwell time of 31.25 kgf and 15 s, respectively. An average of eight readings has been reported here. Retained austenite content in the heat-treated samples was measured by PROTO iXRD retained austenite measuring system using Cr $K\alpha$ radiation. The (211) and (200) reflections of martensite, and (220) and (200) reflections of austenite were used for retained austenite estimation. Metallography was performed on heat-treated samples using two etchants to selectively etch matrix and carbides. *Etchant-1*: 1 g CrO_3 , 100 mL H_2O , and 10 g picric acid (Electrolytic etch: 2–3 V, 30 °C, 30 s); and *etchant-2*: 5

S. Chenna Krishna, Narendra Kumar Gangwar, Abhay K. Jha, Bhanu Pant, and Koshy M. George, Materials and Mechanical Entity, Vikram Sarabhai Space Centre, Trivandrum 695022, India. Contact e-mail: chenna.sk@gmail.com.

drops HCl and 100 mL methanol (Immersion: 15-60 s, 30 °C) were used to etch carbides as dark and colored, respectively. Duly etched samples were examined under an optical microscope and scanning electron microscope equipped with an energy dispersive x-ray spectroscopy (EDS). Thin foils for transmission electron microscopy (TEM) were prepared by cutting 300 μm slices which were reduced to about 100 μm by mechanical polishing. Disks of 3 mm diameter were punched, and one side of the 3 mm disk was dimpled followed by ion milling with an incident beam angle of 4° using GATAN PIPS system. The ion-milled thin foils were examined under a JEOL transmission electron microscope equipped with EDS operated at 200 kV.

3. Results

3.1 Hardness

The effect of hardening temperature on the hardness of the steel is shown in Fig. 1a. The hardness of the samples was in the range of 577-620 HV. Peak hardness of 620 HV was observed at 1000 °C which decreased thereafter with a minimum of 577 HV at 1100 °C. Therefore, 1000 °C was chosen as optimum hardening temperature and subsequent heat treatments were performed on these samples. Figure 1b shows the influence of cryo treatment and tempering on the hardness on the hardened samples. The as-hardened sample showed the maximum hardness of 620 HV. Cryo treatment at -80 °C for 2 h has shown reduction in hardness with a value of 580 HV. Cryo treatment and tempering of the hardened samples resulted hardness in the range of 446-595 HV. Tempering at 180 °C for 2 h has shown slightly lower hardness with a value of 570 HV. Further, drop in hardness was observed at 250 °C with hardness of 554 HV. An increase in hardness was observed with a value of 577 and 595 HV at 500 and 525 °C, respectively. At higher tempering temperature (550-575 °C), a decrease in hardness was observed with minimum of 446 HV at 575 °C. The reason for this variation in hardness with cryo treatment and tempering will be discussed in the sections to follow.

3.2 Retained Austenite (RA)

The influence of different heat treatments (cryo treatment and tempering) on the amount of the retained austenite in the steel is shown in Fig. 2. The hardened sample showed a retained austenite of 9.2%. Upon cryo treatment, the RA% reduced to 8.2% due to transformation of retained austenite to martensite. Tempering of hardened and cryo-treated sample has led to increase in RA%. Tempering at 250 °C has slightly increased the RA% with a value of 10.48%. At 500 and 575 °C, the RA% has significantly increased to 14 and 17%, respectively. Increase in RA% at higher tempering temperature is attributed to formation of reversed austenite as reported for MSSs (Ref 10, 11).

3.3 Optical Microscopy

Figure 3 shows the optical micrographs of the steel in three heat treatment conditions. The optical micrograph shown in Fig. 3a was obtained from hardened sample which comprises

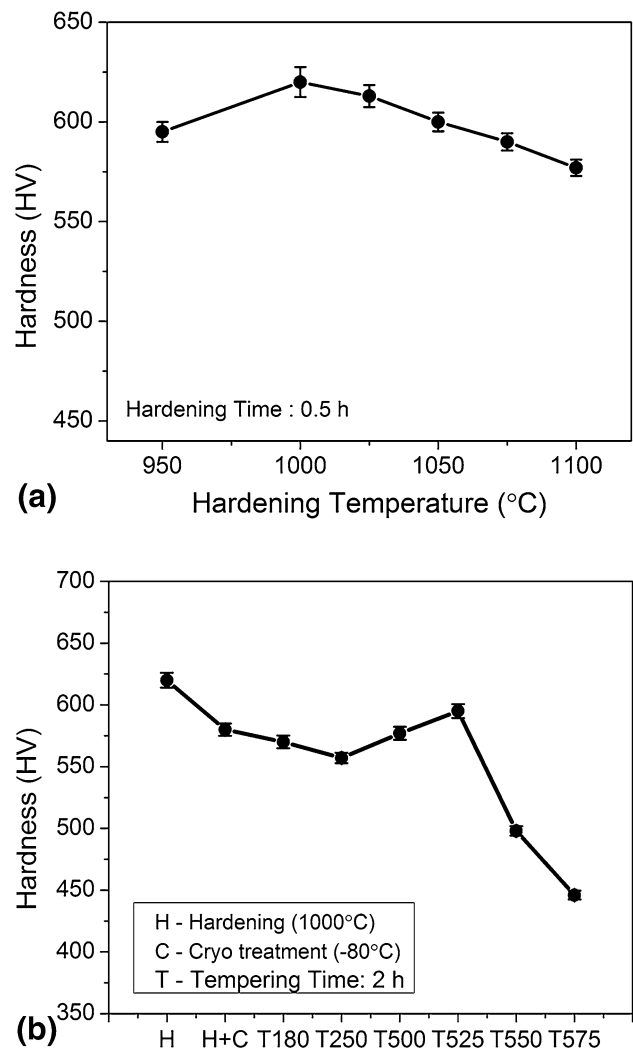


Fig. 1 Effect of heat treatment on the hardness of the steel: (a) hardened, and (b) hardened, cryo treated, and tempered

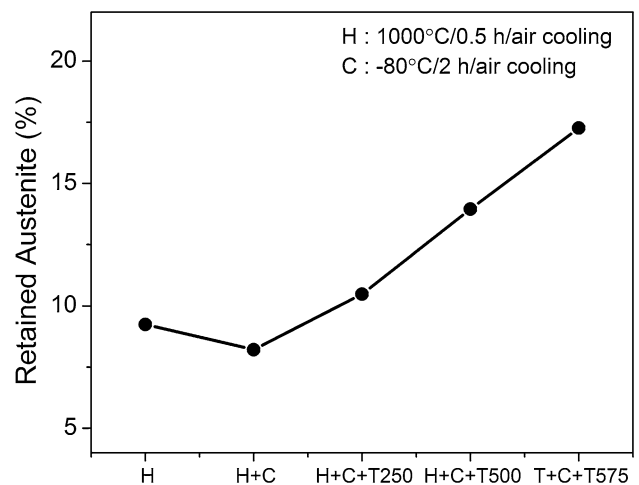


Fig. 2 Influence of hardening, cryo treatment, and tempering on the amount of retained austenite in the steel

martensite and carbides. The carbides were observed as stringers and indicated by arrows. Even though cryo treatment at $-80\text{ }^{\circ}\text{C}$ for 2 h is expected to change the morphology of the martensite, no changes were observed in the optical micrograph as shown in Fig. 3b. On tempering at $500\text{ }^{\circ}\text{C}$ for 2 h, the structure has altered to tempered martensite (Fig. 3c). Selective etching was performed to reveal the carbides in the steel. Figure 3d shows the morphology and distribution of carbides in the martensite matrix at higher magnification. In addition to large spherical primary carbides with thick dark outlines, fine secondary carbides were also observed as gray particles. In order to analyze the phases which were beyond the resolution of optical microscope, electron microscopy was employed.

3.4 Scanning Electron Microscopy

Figure 4 shows the SEM micrograph of the hardened and tempered ($500\text{ }^{\circ}\text{C}$ for 2 h) sample selectively etched to reveal carbides. Figure 4a depicts the primary carbides with average size of $3 \pm 1\text{ }\mu\text{m}$ in the martensite matrix. The EDS spectra obtained from the matrix and carbides are shown in Fig. 4b and c, respectively. Prominent peaks of Fe with peaks of Cr and Mo were observed, confirming to the composition of the matrix as shown in Fig. 4b. On the other hand, EDS spectrum from the carbides showed prominent peaks of Cr and Fe along with peaks of Mo and C. The quantitative analysis result confirms that the carbides are M_7C_3 type with the chemical formula $(\text{Fe,Cr,Mo})_7\text{C}_3$.

3.5 Transmission Electron Microscopy

TEM micrographs obtained from the hardened sample are shown in Fig. 5. The bright field (BF) image shows the lath martensite with high dislocation density, fine carbonitrides ($\text{M}(\text{C,N})$), and M_{23}C_6 carbides (Fig. 5a). The retained austenite is seen as thin films at the lath boundaries as indicated by the arrows in Fig. 5b. In addition to martensite and retained austenite, coarse carbides with an average size of $1.3 \pm 0.2\text{ }\mu\text{m}$ were observed as shown in Fig. 5c. The typical energy dispersive x-ray spectrum (EDS) obtained from the carbide shows prominent peaks of Nb and V, confirming to MC type of carbides (where M is Nb, V) (Fig. 5d). Cryo treatment and low-temperature tempering did not cause any significant change in the microstructure.

After cryo treatment and high-temperature tempering (HTT) at $500\text{ }^{\circ}\text{C}$ for 2 h, precipitation of new phases was observed, in addition to primary carbides. Two types of phases were observed: (i) needle-type precipitates, and (ii) fine spherical precipitates. The needle-type precipitates are mostly seen at the austenite boundaries. The BF image and corresponding selected area diffraction (SAD) pattern from the needle-type precipitates are shown in Fig. 6a and b, respectively. The solved SAD pattern with distinct spot reflections from both martensite matrix and precipitate is shown in Fig. 6c. The precipitates were identified as Cr_2N with HCP crystal structure in the BCC martensite matrix. Figure 7a shows fine spherical particles in the matrix with an average size of $7 \pm 2\text{ nm}$. The SAD pattern

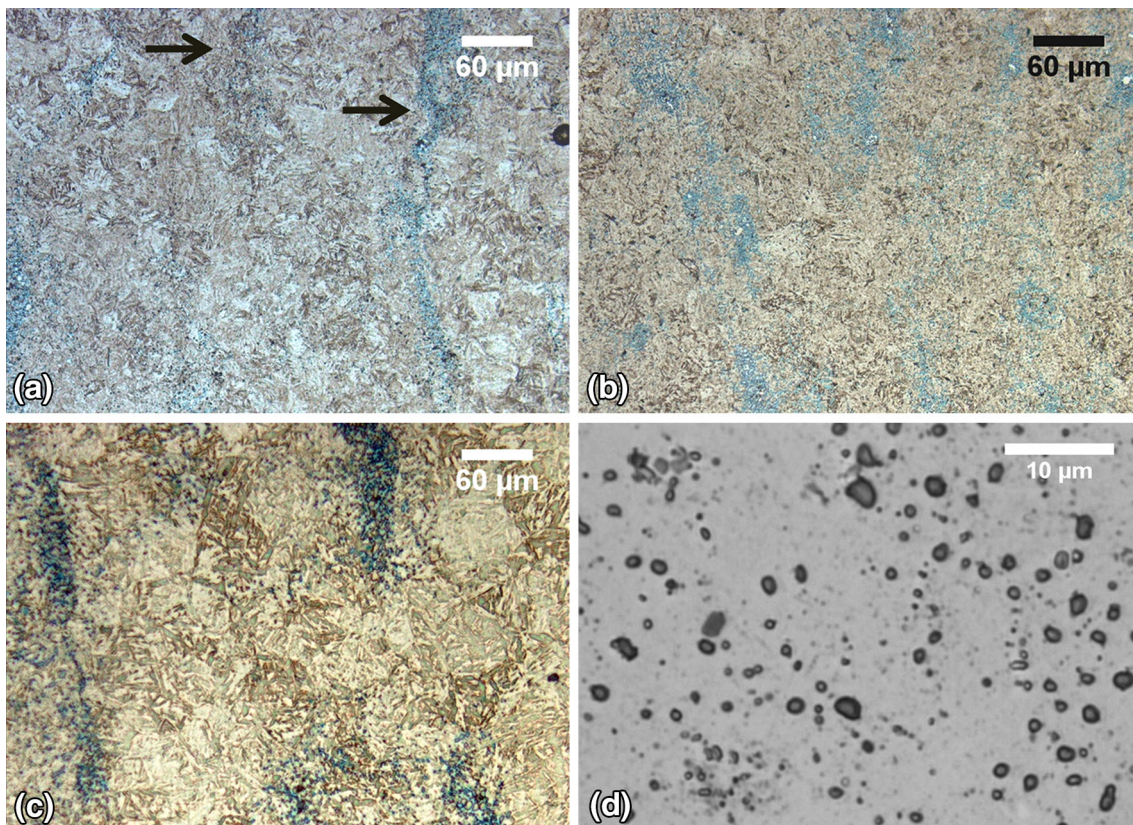


Fig. 3 Effect of heat treatment on the microstructure of the steel (a) hardened (etchant-1), (b) cryo treated (etchant-1), (c) tempered at $500\text{ }^{\circ}\text{C}$ (etchant-1), and (d) tempered at $500\text{ }^{\circ}\text{C}$ at higher magnification (etchant-2)

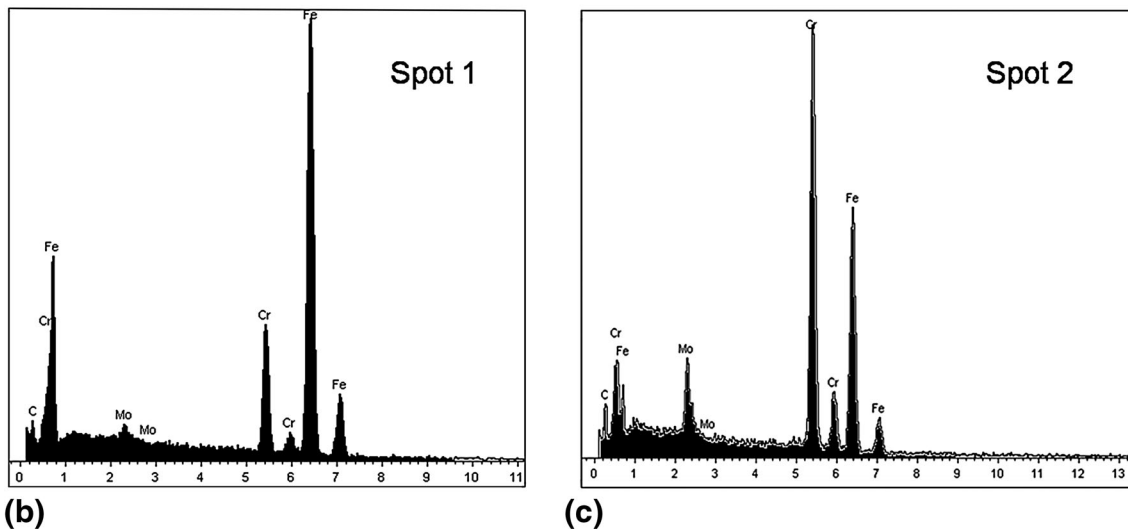
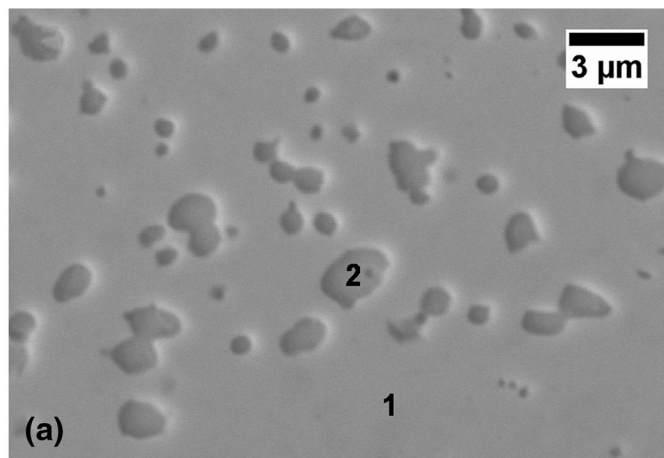


Fig.4 Scanning electron micrographs and energy dispersive spectroscopy spectrum of the steel in the hardened and tempered condition (etchant-2): (a) SEM image, (b) EDS spectrum of the matrix, and (c) EDS spectrum of the carbides

obtained from the spherical particles is shown in Fig. 7b. The spot reflections from the particles and matrix are indicated by ‘P’ and ‘M,’ respectively. The particles were identified as Mo_2C carbides with HCP crystal structure.

4. Discussion

The main constituents of the microstructure in the hardened condition as characterized by optical and electron microscopy were martensite, retained austenite, coarse MC and M_7C_3 carbides, fine carbonitrides of Nb and V, and M_{23}C_6 carbides. The average size of the primary carbides as measured from SEM micrographs was $3 \pm 1 \mu\text{m}$ which is finer than carbides observed in AISI 440C steel (Ref 12). This difference in carbide size between present steel and AISI 440C steel can be attributed to variation in the carbide content in the steel. Higher carbon content of 1 wt.% as observed in the AISI 440C steel, from an isothermal section of Fe-Cr-C phase diagram will result in martensite and large M_7C_3 carbides (Ref 12). On the other hand, medium carbon content (0.38 wt.%) will yield in martensite and fine M_7C_3

carbides as observed in the present steel (Ref 13, 14). In the present steel, the carbon content was 0.45 wt.%, and the rest of the carbon was replaced with nitrogen (0.17 wt.%N) to meet the requirement of high hardness. Upon tempering at 500 °C, two types of fine particles were observed in the martensite matrix: fine spherical Mo_2C carbides and needle-shaped Cr_2N nitrides. Similar type of carbides and nitrides has been reported for stainless steels containing N, Mo, and C (Ref 15-18).

From Fig. 1, it can be ascertained that hardening, cryo treatment, and tempering temperature will influence the hardness of the steel. The reason for the variation in the hardness with hardening temperature is due to change in the volume fraction of carbides and retained austenite. It is reported that M_{23}C_6 carbides dissolve in the temperature range of 950-1050 °C, whereas M_7C_3 carbides dissolve much high temperature (1050-1150 °C) (Ref 13). Increase in the hardening temperature results in dissolution of carbides increasing the alloy content of the austenite and reduces the martensite transformation range (Ref 10, 15). For the present steel, maximum hardness of 620 HV was observed in the sample hardened at 1000 °C which is attributed to partial dissolution of the carbides and carbonitrides, resulting in a minimal amount of

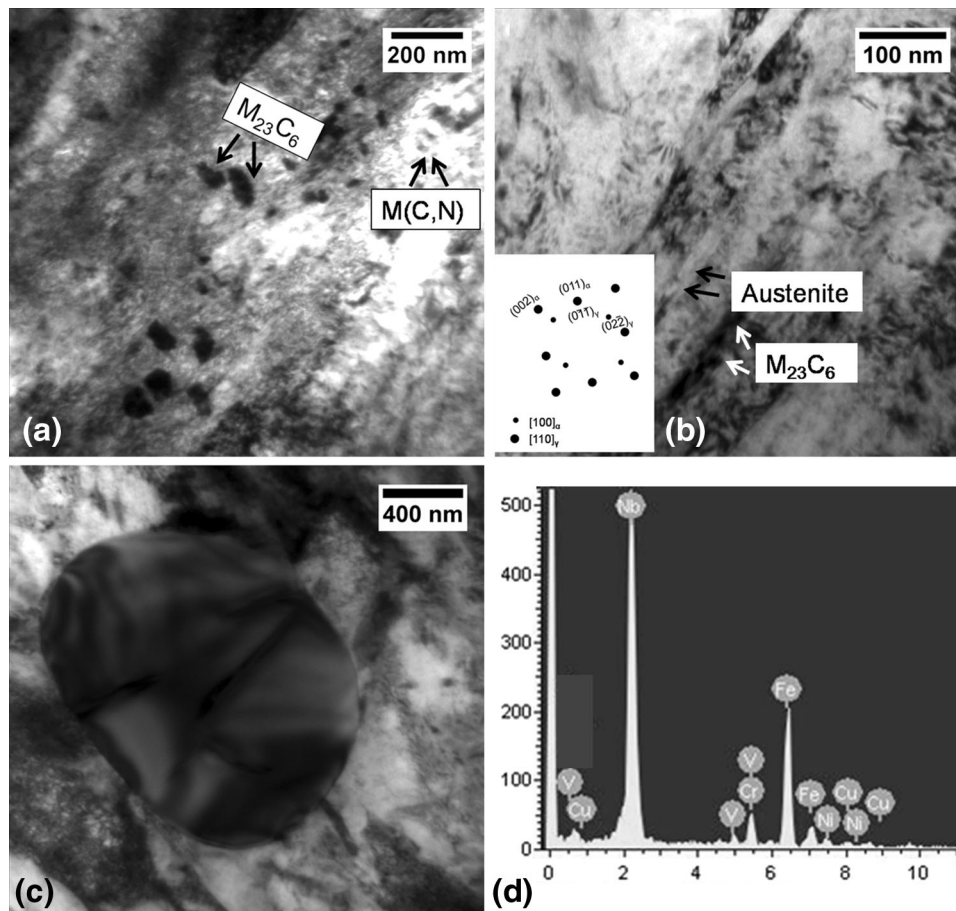


Fig. 5 Transmission electron microscopy images of the steel in hardened condition: (a) bright field image showing carbides and carbonitrides, (b) bright field image showing carbides and retained austenite, (c) bright field image showing large carbide, and (d) EDS spectrum from the large carbide

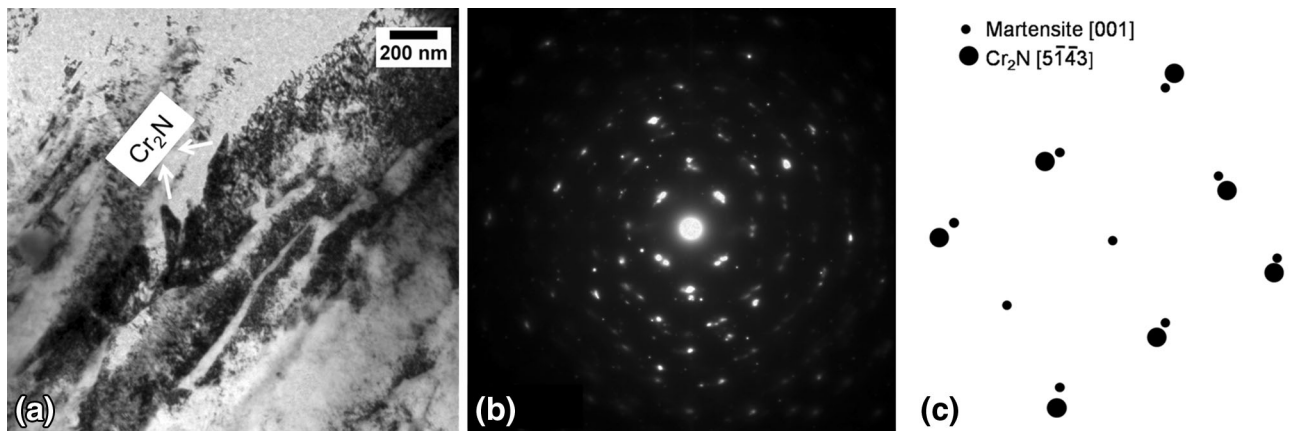


Fig. 6 TEM image and selected area diffraction pattern of the steel in the hardened and tempered (500 °C) condition: (a) bright field image, (b) selected area diffraction (SAD) pattern, and (c) solved SAD pattern

retained austenite (9.2%). At the temperature above 1000 °C, the carbide dissolution might have led to increase in the content of retained austenite resulting in an effective decrease in hardness. Our result agrees with the hardness trend reported for a medium carbon steel (AISI 420) with increasing hardening temperature (Ref 13).

The high hardness of 620 HV observed in the hardened condition is due to solid solution strengthening (Cr, C, and N), dispersion strengthening (carbides and carbonitrides), internal stresses, and high dislocation density. Cryo treatment of the hardened steel led to minor decrease ($\approx 6\%$) in hardness. Similarly, decreasing trend was reported for 815M17 steel in

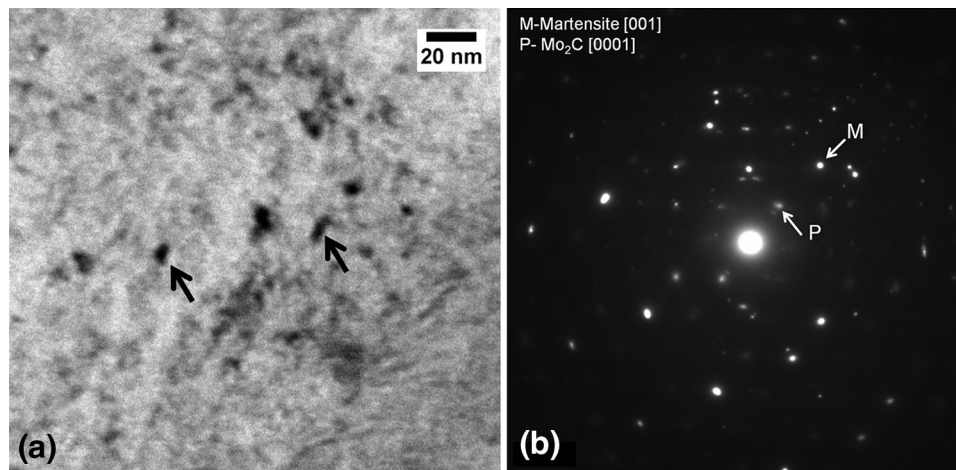


Fig. 7 TEM image and selected area diffraction pattern of the steel in the hardened and tempered (500 °C) condition: (a) bright field image (arrows pointing the precipitates), (b) selected area diffraction pattern

tensile strength after cryo treatment (Ref 19). Nevertheless, the reason for such behavior was not discussed. In addition, most of the studies on cryo treatment of steels reported properties after cryo treatment and tempering (Ref 20, 21). The possible reasons for minor decrease in hardness after cryo treatment are reduction in residual stresses (Ref 20), decomposition of the primary martensite and nucleation of fine carbides (Ref 21), migration and segregation of carbon, nitrogen, and alloying elements at the defects due to lattice distortion, and thermodynamic instability (Ref 22). Nucleation of carbides and migration of carbon and nitrogen are expected to reduce the amount of C and N in martensite matrix with resultant decrease in hardness. Cryo treatment and low-temperature tempering (180 and 250 °C) have resulted in further reduction in hardness (557–570 HV) which may be attributed to (i) increase in the amount of retained austenite (10.4%) compared to hardened (9.2%) and cryo-treated (8.2%) samples, (ii) decrease in internal stresses and dislocation density. HTT at 500 and 525 °C improved the hardness compared to low-temperature tempered samples. The improvement in hardness is due to precipitation of nitrides (Cr_2N) and fine carbides (Mo_2C) as shown in Fig. 6 and 7, respectively. Even though higher retained austenite (14%) is expected to reduce the hardness, fine precipitates are believed to significantly contribute to hardness. Fine carbides and nitrides will contribute to hardness by acting as barriers for dislocation motion and induce secondary hardening resulting in an increased hardness (595 HV). Further, increase in tempering temperature (575 °C) led to decrease in hardness (446 HV) which may be attributed to coarsening of the fine carbides and nitrides, and increase in the volume fraction of retained austenite (17%).

5. Conclusions

1. The main constituents of the steel in hardened condition at 1000 °C for 0.5 h and air cooled were lath martensite, retained austenite, M_{23}C_6 , M_7C_3 , MC carbides, and M(C,N) carbonitrides.
2. Upon cryo treatment (−80 °C for 2 h) and tempering (500 °C for 2 h), two new phases have precipitated fine spherical Mo_2C , and needle-shaped Cr_2N .
3. The hardened steel showed a hardness of 620 HV, where-

as cryo treatment and tempering in the temperature range of 180–250 °C imparted softening and showed hardness in the range of 557–570 HV.

4. Hardening, cryo treatment, and tempering in the temperature range of 500–525 °C have resulted in improved hardness (577–595 HV) due to secondary hardening by precipitation of Mo_2C and Cr_2N particles.
5. The reduction in hardness after tempering at 575 °C may be attributed to formation of reversed austenite and coarsening of carbides and nitrides.

Acknowledgments

The authors would like to thank their colleagues at Material Characterization Division, VSSC for their support in the characterization of the samples. The authors would also like to express sincere gratitude to the Director, VSSC for his kind permission to publish this work.

References

1. H.K.D.H. Bhadeshia, Steels for Bearings, *Prog. Mater. Sci.*, 2012, **57**, p 268
2. K.H. Lo, C.H. Shek, and J.K.L. Lai, Recent Developments in Stainless Steels, *Mater. Sci. Eng. R Rep.*, 2009, **65**, p 39
3. A.K. Jha, M. Swathi Kiranmayee, P. Ramesh Narayanan, K. Sree Kumar, and P.P. Sinha, Metallurgical Analysis of Ball Bearing Seized During Operation, *J. Mater. Eng. Perform.*, 2011, **21**, p 1076
4. K. Clemons, C. Lorraine, G. Salgado, and J. Ogren, Effects of Heat Treatments on Steels for Bearing Applications, *J. Mater. Eng. Perform.*, 2007, **16**, p 515
5. R.J. Parker, and E.N. Bamberger, *Effect of Carbide Distribution on Rolling-Element Fatigue Life of AMS 5749*, NASA-TP-2189, 1983, p 1–15
6. M.A. Ragen, D.L. Anthony, and R.F. Spitzer, A Comparison of the Mechanical and Physical Properties of Contemporary and New Alloys for Aerospace Bearing Applications, *ASTM Special Tech. Publ.*, 2002, **1419**, p 362–374
7. S. Tanaka, K. Yamamura, and M. Oohori, The Development of Bearing Steels with Long Life and High Corrosion Resistance, *ASTM Special Tech. Publ.*, 2002, **1419**, p 414–426
8. X.P. Ma, L.J. Wang, B. Qin, C.M. Liu, and S.V. Subramanian, Effect of N on Microstructure and Mechanical Properties of 16Cr5Ni1Mo Martensitic Stainless Steel, *Mater. Des.*, 2012, **34**, p 74

9. L. Sun, J. Li, L. Zhang, S. Yang, and Y. Chen, Production of Nitrogen-Bearing Stainless Steel by Injecting Nitrogen Gas, *J. Iron Steel Res. Int.*, 2011, **18**, p 7
10. W. Jiang, D. Ye, J. Li, J. Su, and K. Zhao, Reverse Transformation Mechanism of Martensite to Austenite in 00Cr15Ni7Mo2WCu2 Super Martensitic Stainless Steel, *Steel Res. Int.*, 2013, **85**(7), p 1150–1157
11. N. Zhu, Q. Wu, Y. He, X. Lu, L. Li, and P. Hu, Effect of Ni on the Stability of Retained Austenite and Mechanical Properties for TRIP Steels Containing Vanadium, *Steel Res. Int.*, 2014, **85**, p 2
12. D.W. Hetzner and W. Van Geertruyden, Crystallography and Metallography of Carbides in High Alloy Steels, *Mater. Charact.*, 2008, **59**, p 825
13. L.D. Barlow and M. Du Toit, Effect of Austenitizing Heat Treatment on the Microstructure and Hardness of Martensitic Stainless Steel AISI, 420, *J. Mater. Eng. Perform.*, 2011, **21**, p 1327
14. T. Wen, X. Hu, Y. Song, D. Yan, and L. Rong, Carbides and Mechanical Properties in a Fe-Cr-Ni-Mo High-Strength Steel with Different V Contents, *Mater. Sci. Eng. A*, 2013, **588**, p 201
15. A.J. Ramirez, J.C. Lippold, and S.D. Brandi, The Relationship Between Chromium Nitride and Secondary Austenite Precipitation in Duplex Stainless Steels, *Metall. Mater. Trans. A*, 2003, **34**, p 1575
16. S. Chenna Krishna., N.K. Gangwar, A.K. Jha, B. Pant, and K.M. George, Microstructure and Properties of 15Cr-5Ni-1Mo-1W Martensitic Stainless Steel *Steel Res. Inter.*, 2015, **86**, p 51
17. S. Chenna Krishna, J. Srinath, A.K. Jha, B. Pant, S.C. Sharma, and K.M. George, Effect of Heat Treatment on Microstructure and Mechanical Properties of 12Cr-10Ni-0.25 Ti-0.7 Mo Stainless Steel, *Metallogr. Microstruct. Anal.*, 2013, **2**, p 234
18. A. Rajasekhar, G. Madhusudhan Reddy, T. Mohandas, and V.S.R. Murti, Influence of Austenitizing Temperature on Microstructure and Mechanical Properties of AISI, 431 Martensitic Stainless Steel Electron Beam Welds, *Mater. Des.*, 2009, **30**, p 1612
19. A. Bensely Senthilkumar, D. Senthilkumar, D. Mohan Lal, G. Nagarajan, and A. Rajadurai, Effect of Cryogenic Treatment on Tensile Behavior of Case Carburized Steel-815M17, *Mater. Charact.*, 2007, **58**, p 485
20. Paolo Baldissera and Cristiana Delprete, Deep Cryogenic Treatment: A Bibliographic Review, *Open Mech. Eng. J.*, 2008, **2**, p 1
21. Nirmal S. Kalsi, Rakesh Sehgal, and Vishal S. Sharma, Cryogenic Treatment of Tool Materials: A Review, *Mater. Manuf. Process.*, 2010, **25**, p 1077
22. F. Meng, K. Tagashira, R. Azuma, and H. Sohma, Role of Eta-Carbide Precipitations in the Wear Resistance Improvements of Fe-12Cr-Mo-V-1.4 C Tool Steel by Cryogenic Treatment, *ISIJ Int.*, 1994, **34**, p 205